Tellurium Hydrides at High Pressures: High-Temperature Superconductors

Xin Zhong,[1] Hui Wang,[1] Jurong Zhang,[1] Hanyu Liu,[1] Shoutao Zhang,[1] Hai-Feng Song,[4,5]
Guochun Yang,[2,1,*] Lijun Zhang,[3,1,†] and Yanming Ma[1,‡]
[1]*State Key Laboratory of Superhard Materials, Jilin University, Changchun 130012, China*
[2]*Faculty of Chemistry, Northeast Normal University, Changchun 130024, China*
[3]*College of Materials Science and Engineering and Key Laboratory of Automobile Materials of MOE,*
Jilin University, Changchun 130012, China
[4]*Laboratory of Computational Physics, Institute of Applied Physics and Computational Mathematics, Beijing 100088, China*
[5]*CAEP Software Center for High Performance Numerical Simulation, Beijing 100088, China*

(Received 14 April 2015; revised manuscript received 6 November 2015; published 4 February 2016)

Observation of high-temperature superconductivity in compressed sulfur hydrides has generated an irresistible wave of searches for new hydrogen-containing superconductors. We herein report the prediction of high-T_c superconductivity in tellurium hydrides stabilized at megabar pressures identified by first-principles calculations in combination with a swarm structure search. Although tellurium is isoelectronic to sulfur or selenium, its heavier atomic mass and weaker electronegativity makes tellurium hydrides fundamentally distinct from sulfur or selenium hydrides in stoichiometries, structures, and chemical bondings. We identify three metallic stoichiometries of H_4Te, H_5Te_2, and HTe_3, which are not predicted or known stable structures for sulfur or selenium hydrides. The two hydrogen-rich H_4Te and H_5Te_2 phases are primarily ionic and contain exotic quasimolecular H_2 and linear H_3 units, respectively. Their high-T_c (e.g., 104 K for H_4Te at 170 GPa) superconductivity originates from the strong electron-phonon couplings associated with intermediate-frequency H-derived wagging and bending modes, a superconducting mechanism which differs substantially with those in sulfur or selenium hydrides where the high-frequency H-stretching vibrations make considerable contributions.

DOI: 10.1103/PhysRevLett.116.057002

A recent breakthrough finding in the field of superconductivity is the observation of remarkable high-temperature superconductivity (T_c up to 203 K) in hydrogen sulfide (H_2S) under pressure [1]. This was achieved by a direct investigation on a theoretical prediction of high-T_c superconductivity in compressed solid H_2S within the framework of Bardeen-Cooper-Schrieffer (BCS) theory [2,3]. The superconductive mechanism of H_2S and its possible decomposition at high pressures were then explored extensively [4–9]. Besides these efforts, other new superconductors have been sought in relevant hydrogen-containing compounds. Selenium (Se) hydrides have been predicted to exhibit high T_c in the range of 40–131 K at megabar pressures [10,11].

Tellurium (Te) is the next group-VIA element isoelectronic to S and Se. Its larger atomic core and weaker electronegativity than S and Se means that Te will exhibit a rather different chemistry. For instance, H_2S [12] and H_2Se [13] are stable as gas molecules and as solids at ambient pressure, but H_2Te gas molecules are unstable and rapidly decompose into the constituent elements (above −2 °C) [14]. Thus far, no stable solidified Te hydride has been reported.

Pressure can fundamentally modify the chemical reactivity of an element or compound. For instance, it can overcome the reaction barrier of hydrogen and certain substances to form stable hydrides (*e.g.*, noble metal hydrides [15,16], LiH_6 [17], NaH_9 [18], and CaH_6 [19], etc.). Thus, high pressure may allow Te hydrides to be synthesized from a mixture of Te and H_2. As to the superconductivity, on one hand one may argue that Te hydrides may not be good candidates for high-T_c superconductors because the low Debye temperature caused by Te with high atomic mass might suppress the superconductivity. On the other hand, low-frequency vibrations (soft phonons) associated with heavy Te can enhance electron-phonon coupling (EPC) [20], as seen from the higher T_c (up to 80 K) predicted for SnH_4 [21] than for SiH_4 (up to 17 K) [22] and GeH_4 (up to 64 K) [23].

We herein extensively explore the high-pressure phase diagram of Te hydrides by using the swarm-intelligence based structural prediction calculations [24,25]. Distinct from S and Se hydrides, Te hydrides exhibit a unique potential energy landscape, where the unexpected stoichiometries of H_4Te, H_5T_2, and HTe_3 emerge as stable species at megabar pressures. H_4Te is so far the most H-rich stoichiometry reported in the family of chalcogen hydrides. The H-rich H_4Te and H_5T_2 compounds are primarily ionic, and consist of novel quasimolecular H_2 and linear H_3 units, respectively, both of which are metallic and show high-temperature superconductivity with T_c reaching 104 K (i.e., H_4Te at 170 GPa). Our work provides clear guidance for future experimental exploration of potential high-temperature superconductivity in Te hydrides under pressure.

We employ the in-house developed CALYPSO structure prediction method, which is designed to search for the stable structures of given compounds [24,25], for the investigation of phase stability of Te hydrides at high pressures. The details of the search algorithm and its applications are described elsewhere [24,26–28]. The underlying energetic calculations are performed with the plane-wave pseudopotential method as implemented in the VASP code [29]. The Perdew-Burke-Ernzerhof generalized gradient approximation [30] is chosen for the exchange-correlation functional. The electron-ion interaction is described by projector-augmented-wave potentials with the $1s^1$ and $5s^25p^4$ configurations treated as valence electrons for H and Te, respectively. During the structure search, an economy set of parameters is used to evaluate the relative enthalpies of the sampled structures on the potential energy surface; a kinetic cutoff energy of 500 eV and Monkhorst-Pack k meshes with grid spacing of $2\pi \times 0.03$ Å^{-1} are then adopted to ensure the enthalpy converges to better than 1 meV/atom. The phonon spectrum and EPC of the stable compounds are calculated within the framework of linear response theory through the Quantum-ESPRESSO code [31].

We focus our structure search on H-rich compounds that are promising candidates for higher-T_c superconductivity [32]. The energetic stabilities of a variety of H_xTe_y ($x = 1$–8 and $y = 1$–3) compounds are evaluated by their formation enthalpies relative to the products of dissociation into constituent elements (ΔH) at 0, 50, 100, 200, and 300 GPa, as depicted in Fig. 1 and the Supplemental Material [33]. At 0 GPa, no stoichiometry is stable against elemental dissociation, consistent with the fact that there is no solid H-Te phase at ambient conditions. This situation preserves up to 100 GPa, but accompanied with greatly decreased ΔH magnitudes, implying a tendency of H-Te compounds being stabilized under further compression. Indeed, at 200 GPa, all the stoichiometries become energetically favored over elemental dissociation, and stable stoichiometries of H_4Te, H_5Te_2, and HTe emerge on the convex hull. At 300 GPa, in addition to these three species, another stable stoichiometry of HTe_3 appears in the H-poor regime. Finding these unexpected stable H-Te stoichiometries is distinct from the actual stabilization of H_3S/H_3Se, HS/HSe, and HS_2/HSe_2 in S and Se hydrides [see Fig. 1(a)] [9,10]. As discussed later, all four stable H-Te compounds are metallic in their stable pressure regions [Fig. 1(b)].

The most H-rich stoichiometry, H_4Te, was predicted to crystallize at above 162 GPa in a hexagonal structure (space group $P6/mmm$), consisting of H-sharing 12-fold TeH_{12} octahedrons [Fig. 2(a)]. An unusual structural feature of this phase is that the short H-H contact (~0.85 Å at 200 GPa) between two octahedrons forms a quasimolecular H_2 unit. The electron localization function (ELF) between two H atoms within the H_2 unit is high (~0.9), indicating a strong H-H covalent bond. The longer H-H bond length than that of a free H_2 molecule (0.74 Å) is attributed to an accepted charge of ~0.44e per H_2 donated by Te (see the Bader charge analysis of the Supplemental Material [33]), which resides in the H_2 antibonding orbital, and thus lengthens the intramolecular bond. Note that this charge transfer is a prerequisite for forming quasimolecular H units in compressed hydrides, as reported for LiH_n ($n = 2$, 6, and 8) [17], CaH_6 [19], GeH_4 [23], and SnH_4 [21,39]. No electron localization is found between H and Te in the ELF, indicating the ionic nature of H-Te bonding.

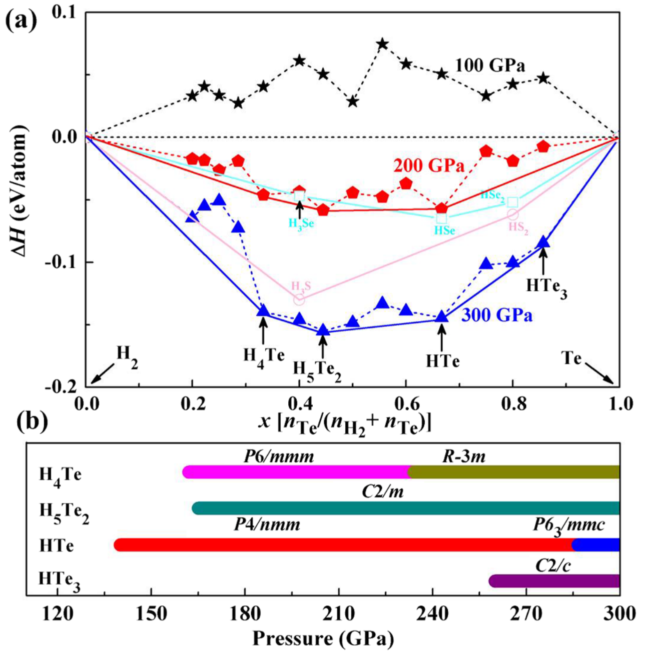

FIG. 1. (a) Formation enthalpies (ΔH) of various H-Te compounds with respect to decomposition into constituent elemental solids at 100–300 GPa. Data points located on the convex hull (solid lines) represent stable species against any type of decomposition. The results of H-S [9] (open circles at 250 GPa) and H-Se [10] (open squares at 300 GPa) systems are shown for comparison. (b) Pressure ranges in which the corresponding structures of different stoichiometries are stabilized. The phases I ($P3_121$), V ($Im-3m$), VI ($I4/mmm$), and VII ($Fm-3m$) of Te [37], and the $P6_3m$ and $C2/c$ structures of solid H_2 [38] are used for calculating ΔH. The hull data remain essentially unchanged with the inclusion of zero-point energies (see the Supplemental Material [33]).

Upon compression, the $P6/mmm$ structure of H_4Te transforms into a more energetically favored R-3m structure at 234 GPa. This is a first-order transition, and it is accompanied by an increase of the coordination number of Te from 12 to 14 with the formation of H-sharing TeH_{14} octadecahedrons [Fig. 2(b)]. There are two types of H atoms that occupy two different 2c Wyckoff sites: atoms labeled H1 are shared by four Te atoms, whereas the H2 atoms are coordinated by three Te atoms and meanwhile bond with another H2 atom to form a quasimolecular H_2 unit with a bond length of ~0.86 Å (at 300 GPa). We found a weak pressure dependence of the intramolecular H-H bond length

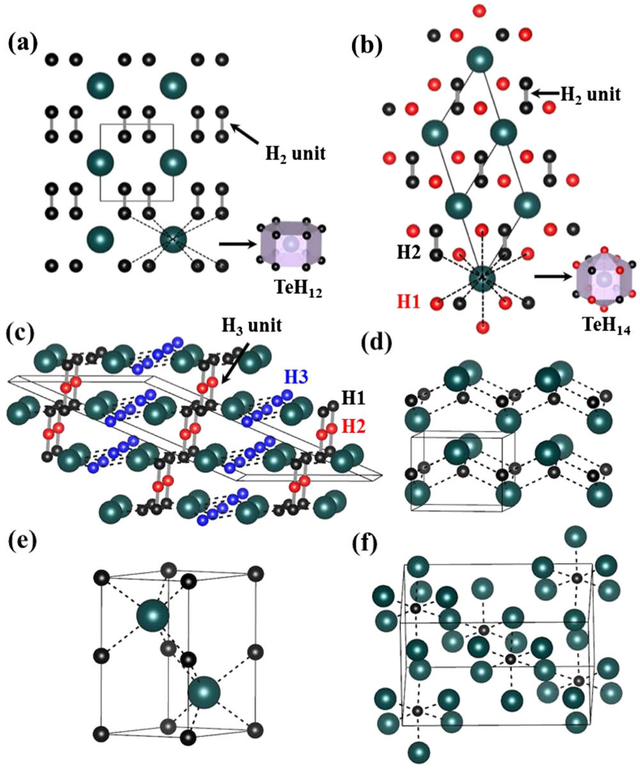

FIG. 2. Structures of stable H-Te compounds at high pressures derived from the CALYPSO structure search: (a),(b) H_4Te in the $P6/mmm$ and $R\text{-}3m$ structures, respectively; (c) H_5Te_2 in the $C2/m$ structure; (d),(e) HTe in the $P4/nmm$ and $P6_3/mmc$ structures, respectively; (f) HTe_3 in the $C2/c$ structure. Small and large spheres represent H and Te atoms. Solid lines depict the unit cells of the structures. See the Supplemental Material [33] for more detailed structural information.

for both the $P6/mmm$ and $R\text{-}3m$ phases, similar to those reported for other compressed hydrides [17,21,23,39].

The energetically favored structure of H_5Te_2 (stable above 165 GPa) has a $C2/m$ symmetry [Fig. 2(c)], consisting of the puckered layers, where Te atoms at the $4i$ sites are threefold coordinated by two inequivalent H atoms (H1 and H3) at also the $4i$ sites. Another type of H atom (H2) at the $2c$ sites is accommodated between two puckered layers and connects with two H1 atoms to form unexpected linear quasimolecular H_3 units. The two H-H covalent bonds in the H_3 unit have lengths of ~0.92 Å, with a maximal bonding ELF of ~0.8 at 200 GPa. The formation of H_3 units is accompanied by a similar charge transfer from Te to H as described above. Note that such linear H_3 units are often found in gas molecules [40–43], but rarely observed in solid phases (*e.g.*, BaH_6 [44] and H-rich Rb compounds [45]).

The next stoichiometry, HTe (stable above 140 GPa), adopts a PbO-type structure [space group $P4/nmm$, Fig. 2(d)] composed of edge-sharing TeH_4-tetrahedron layers, which is isostructural with that of Fe-based superconductor FeSe [46] and Se hydride of HSe [10]. With increasing pressure, a more stable NiAs-type structure [space group $P6_3/mmc$, Fig. 2(e)] emerges at 286 GPa; its coordination number increases from 4 to 6. The H-poor HTe_3 stoichiometry (stable above 260 GPa) adopts a structure of $C2/c$ symmetry [Fig. 2(f)], in which two inequivalent Te atoms (at the $4c$ and $8f$ sites) and H atoms (at the $4e$ sites) form interpenetrating polymeric networks. Each H atom is sixfold coordinated by Te.

The electronic band structure and density of states (DOS) of all the above stable H-Te phases (Figs. 3 and S4) exhibit metallic features. To probe the role Te plays in determining electronic structures of the H-rich species (*e.g.*, H_4Te), we calculate the band structure of a hypothetical H_4Te_0 system by removing the Te from the lattice, leaving the H sublattice unchanged. A uniform compensated background charge ($6e/Te$) is applied to preserve the total valence electrons of the system. The resultant band structure [red dashed lines in Fig. 3(a)] is similar to that of actual H_4Te (solid black lines). This indicates that the Te atoms mainly act as electron donors, consistent with the ionic character of H-Te bonds. This is in sharp contrast to the S and Se hydrides, in which strong covalent $H-S/H-Se$ bonding dominates [4,10]. Both H_4Te and H_5Te_2 [Fig. 3(b)] show a strong DOS peak originating from Te-p and substantial H-derived states around the Fermi level (E_f). A "flat band-steep band" feature [47] appears around the E_f [Fig. 3(a)]. These

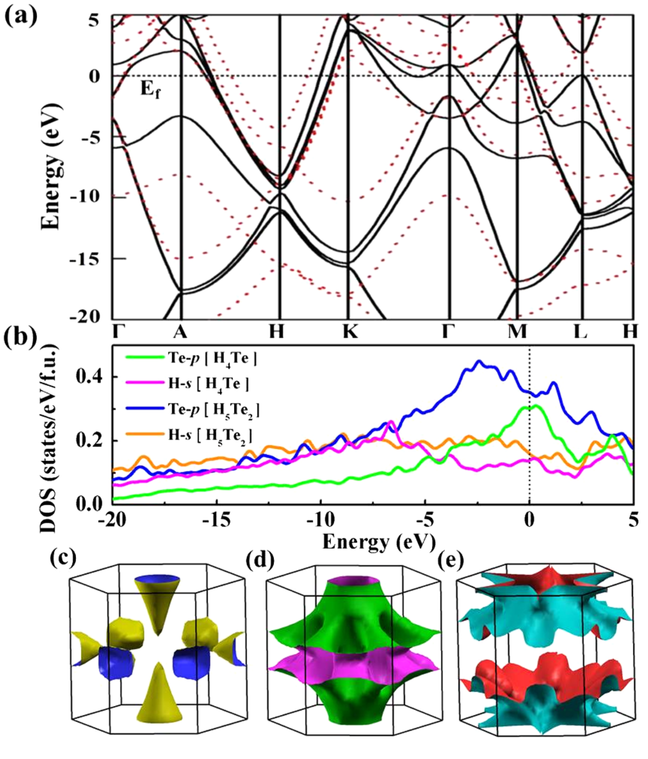

FIG. 3. (a) Electronic band structure of H_4Te in the $P6/mmm$ structure at 200 GPa. The red dashed lines represent the band structure of the H sublattice with a uniform compensated background charge. (b) Projected density of states for H_4Te and H_5Te_2 in the $C2/m$ structure at 200 GPa. (c)–(e) Fermi surfaces of H_4Te.

are typical features that favor strong EPC, and thus high-T_c superconductivity. The Fermi surface of H_4Te [Figs. 3(c)–3(e)] does not show any visible nesting feature. The evaluated carrier concentration parameter, r_s [48], of H_4Te and H_5Te_2 at 200 GPa are 5.20 and 4.05, respectively. These values are comparable to those of alkali metals (3.2–5.7), but much higher than that of the hypothetical monoatomic phase of solid hydrogen (1.6) [49].

We then performed phonon and EPC calculations for three H-rich species of H_4Te, H_5Te_2, and HTe to probe their potential superconductivity. The absence of any imaginary frequency in the phonon spectra clearly indicates the dynamical stability of all the predicted H-Te phases. The calculated EPC parameters, λ, for H_4Te, H_5Te_2, and HTe at 200 GPa are 1.46, 1.14, and 0.58, respectively. The λ values of H_4Te and H_5Te_2 are comparable to those predicted for H_2S [2] and H_3S/H_3Se [4,10], indicating fairly strong EPC in the Te hydrides. Interestingly, λ decreases almost linearly with decreasing H content in the order of $H_4Te >$ $H_5Te_2 >$ HTe (see the Supplemental Material [33]). This underlies the dominant role of H involvement in controlling the EPC of H-containing materials [32].

Figure 4 shows the projected phonon DOS, Eliashberg EPC spectral function $\alpha^2F(\omega)$, and its integral $\lambda(\omega)$ for H_4Te and H_5Te_2. For the $P6/mmm$-H_4Te [Fig. 4(a)], the low-frequency translational vibrations from the heavy Te atoms (below 10 THz) contribute 22% of the total λ. The high-frequency stretching modes associated with the quasimolecular H_2 units (70–80 THz) contribute only 5% of λ. The main contributor to the EPC (72% of λ) originates from the midfrequency H-Te wagging and H-Te-H bending vibrations (10–50 THz). Similarly, for the R-$3m$-H_4Te [Fig. 4(b)], the mid-lying H wagging and bending modes contribute 73% of the total λ, whereas the high-lying vibrations from H_2 units contribute only 3%. A similar trend applies to H_5Te_2 [Fig. 4(c)], where the contribution of the high-lying vibrations of the linear H_3 units to the total λ is quite small (<5%). These results highlight that midfrequency H-derived phonons and low-frequency vibrations from Te atoms are mainly responsible for the EPC in the H-Te systems. The involvement of massive Te atoms softens these phonon modes, from which the strong EPCs originate. This superconductive mechanism is not unusual by seeing those in SnH_4 [21,33] and CaH_6 [19] that contain similar quasimolecular H_2/H_4 units. However, the mechanism is apparently different to that in H-S and H-Se systems, where the high-frequency H-stretching vibrations make a large contribution to the overall EPC [2,4,10]. This distinctive EPC feature is clearly reflected in the different phonon linewidth data shown by H_4Te vs H_3S/H_3Se (as shown in the Supplemental Material [33]).

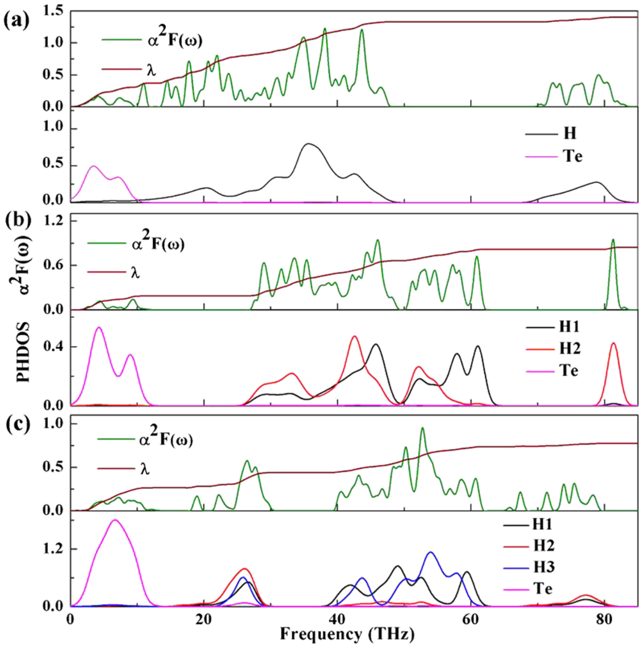

FIG. 4. Calculated projected phonon density of states (lower panels), Eliashberg EPC spectral function $\alpha^2F(\omega)$ and its integral $\lambda(\omega)$ (upper panels) of (a) H_4Te ($P6/mmm$) at 200 GPa, (b) H_4Te (R-$3m$) at 300 GPa, and (c) H_5Te_2 ($C2/m$) at 300 GPa.

The superconducting T_c of the predicted stable H-rich compounds is evaluated through the Allen-Dynes modified McMillan equation [50] by using the calculated logarithmic average frequency, $\omega_{\log}$, and a series of Coulomb pseudopotential parameters, $\mu*$, from 0.1 to 0.2 [51] (as summarized in the Supplemental Material [33]). At $\mu* = 0.1$, the resultant T_c values are 99, 58, and 19 K for H_4Te, H_5Te_2, and HTe at 200 GPa, respectively. The highest T_c of H_4Te is attributed to its strong EPC ($\lambda = 1.46$) and high $\omega_{\log}$ (929.1 K). For H_4Te and H_5Te_2, we find a negative pressure dependence of T_c. This results from the decrease of λ under compression, even though $\omega_{\log}$ increases due to phonon hardening. In the established stable pressure regions for all the phases [Fig. 1(b)], the maximum T_c of 104 K using $\mu* = 0.1$ (or 95 K for $\mu* = 0.13$) occurs in H_4Te at 170 GPa. The actual T_c may be enhanced further as a result of the multiband effect [52,53] given the different kinds of Fermi surface sheets shown in Figs. 3(c)–3(e).

Although Te is isoelectronic to S and Se, we hereby observe entirely different stoichiometries and stable structures of compressed Te hydrides compared with S/Se hydrides. Two novel stable stoichiometries of H_4Te and H_5Te_2, with exotic quasimolecular H_2/H_3 units, are identified; they are not seen in S/Se hydrides [9,10]. This sharp distinction originates from the fundamentally different chemical bonding of the H–Te system from that in H – S/H – Se. The S and Se have smaller atomic cores and larger Pauling electronegativities (2.58 and 2.55) than Te, and thus are favorable for forming strong covalent bonds with H in S/Se hydrides. In contrast, in the Te hydrides, owing to the larger atomic core of Te and its smaller electronegativity (2.1), substantial charge transfers from Te to H. As a result, the H-Te bond is primarily ionic.

Upon appearance of the additional charges on the anionic H atoms, substantial energy can be reduced via the formation of H-H covalent bonds. This may be the physical mechanism of the stabilization of the quasimolecular H_2/H_3 units in the H-rich compounds. The existence of these quasimolecular units accommodates more H, and thus explains the emergence of the highest known H content in H_4Te of any chalcogen hydride.

The two H-rich hydrides (H_4Te and H_5Te_2) are promising superconductors, with predicted T_c of up to 104 and 58 K, respectively. The EPC feature responsible for the superconductivity is substantially different from that in superconducting S/Se hydrides. We expect that our predictions of stable Te hydrides and their superconducting properties will stimulate future experimental studies on the synthesis of Te hydrides to probe their high-temperature superconductivity at high pressures. The diverse properties disclosed for Te hydrides here are a useful contribution to our in-depth understanding of the behaviors of superconducting chalcogen hydrides at megabar pressures.

The authors acknowledge the funding supports from National Natural Science Foundation of China under Grants No. 11274136 and No. 11534003, 2012 Changjiang Scholar of Ministry of Education, the National High Technology Research and Development Program of China under Grants No. 2015AA01A304, the Postdoctoral Science Foundation of China under Grant No. 2013M541283 and the fund of CAEP-CSCNS (R2015-03). L. Z. acknowledges funding support from the Recruitment Program of Global Experts (the Thousand Young Talents Plan).

---

[*] Corresponding author.
yanggc468@nenu.edu.cn
[†] Corresponding author.
lijun_zhang@jlu.edu.cn
[‡] Corresponding author.
mym@jlu.edu.cn

[1] A. P. Drozdov , M. I. Eremets, I. A. Troyan, V. Ksenofontov, and S. I. Shylin, Nature (London) **525**, 73 (2015).

[2] Y. Li , J. Hao, H. Liu, Y. Li, and Y. Ma, J. Chem. Phys. **140**, 174712 (2014).

[3] E. Cartlidge, Nature, doi:10.1038/nature.2014.16552 (2014).

[4] D. Duan *et al.*, Sci. Rep. **4**, 6968 (2014).

[5] N. Bernstein , C. S. Hellberg, M. D. Johannes, I. I. Mazin, and M. J. Mehl, Phys. Rev. B **91**, 060511 (2015).

[6] D. Duan , X. Huang, F. Tian, D. Li, H. Yu, Y. Liu, Y. Ma, B. Liu, and T. Cui, Phys. Rev. B **91**, 180502 (2015).

[7] D. A. Papaconstantopoulos , B. M. Klein, M. J. Mehl, and W. E. Pickett, Phys. Rev. B **91**, 184511 (2015).

[8] A. P. Durajski *et al.*, Nature (London) **515**, 73 (2015).

[9] I. Errea, M. Calandra, C. J. Pickard, J. Nelson, R. J. Needs, Y. Li, H. Liu, Y. Zhang, Y. Ma, and F. Mauri, Phys. Rev. Lett. **114**, 157004 (2015).

[10] S. Zhang, Y. Wang, J. Zhang, H. Liu, X. Zhong, H.-F. Song, G. Yang, L. Zhang, and Y. Ma, Sci. Rep. **5**, 15433 (2015).

[11] J. A. Flores-Livas, A. Sanna, and E. K. U. Gross, arXiv: 1501.06336.

[12] M. Collins, C. Ratcliffe, and J. Ripmeester, J. Phys. Chem. **93**, 7495 (1989).

[13] J. H. Loehlin, P. G. Mennitt, and J. S. Waugh, J. Chem. Phys. **44**, 3912 (1966).

[14] D. R. Lide, *CRC Handbook of Chemistry and Physics*, 87th ed. (CRC Press, Boca Raton, FL, 2006), ISBN 0-8493-0487-8493.

[15] G. Gao , H. Wang, L. Zhu, and Y. Ma, J. Phys. Chem. C **116**, 1995 (2012).

[16] D. Y. Kim , R. H. Scheicher, C. J. Pickard, R. J. Needs, and R. Ahuja, Phys. Rev. Lett. **107**, 117002 (2011).

[17] E. Zurek, R. Hoffmann, N. W. Ashcroft, A. R. Oganov, and A. O. Lyakhov, Proc. Natl. Acad. Sci. U.S.A. **106**, 17640 (2009).

[18] P. Baettig and E. Zurek, Phys. Rev. Lett. **106**, 237002 (2011).

[19] H. Wang, J. S. Tse, K. Tanaka, T. Iitaka, and Y. Ma, Proc. Natl. Acad. Sci. U.S.A. **109**, 6463 (2012).

[20] L. R. Testardi. Phys. Rev. B **5**, 4342 (1972).

[21] J. S. Tse, Y. Yao, and K. Tanaka, Phys. Rev. Lett. **98**, 117004 (2007).

[22] M. I. Eremets, I. A. Trojan, S. A. Medvedev, J. S. Tse, and Y. Yao, Science **319**, 1506 (2008).

[23] G. Gao, A. R. Oganov, A. Bergara, M. Martinez-Canales, T. Cui, T. Iitaka, Y. Ma, and G. Zou, Phys. Rev. Lett. **101**, 107002 (2008).

[24] Y. Wang *et al.*, Phys. Rev. B **82**, 094116 (2010).

[25] Y. Wang *et al.*, Comput. Phys. Commun. **183**, 2063 (2012).

[26] Y. Wang H. Liu, J. Lv, L. Zhu, H. Wang, and Y. Ma, Nat. Commun. **2**, 563 (2011).

[27] L. Zhu *et al.*, Nat. Chem. **6**, 644 (2014).

[28] J. Lv Y. Wang, L. Zhu, and Y. Ma, Phys. Rev. Lett. **106**, 015503 (2011).

[29] G. Kresse and J. Furthmuller, Phys. Rev. B **54**, 11169 (1996).

[30] J. P. Perdew J. A. Chevary, S. H. Vosko, K. A. Jackson, M. R. Pederson, D. J. Singh and C. Fiolhais, Phys. Rev. B **46**, 6671 (1992).

[31] P. Giannozzi *et al.*, J. Phys. Condens. Matter **21**, 395502 (2009).

[32] N. W. Ashcroft, Phys. Rev. Lett. **92**, 187002 (2004).

[33] See Supplemental Material at http://link.aps.org/supplemental/10.1103/PhysRevLett.116.057002 which includes Refs. [34–36]. It contains more detailed computational methods, explicit structural information of the identified stable H-Te compounds, as well as additional results on the phase stabilities, zero-point energy effect, Bader charge analysis, electron-phonon coupling feature, superconducting properties, etc.

[34] K. Parlinski, Z-. Q. Li, and Y. Kawazoe, Phys. Rev. Lett. **78**, 4063 (1997).

[35] A. Togo, F. Oba, and I. Tanaka, Phys. Rev. B **78**, 134106 (2008).

[36] P. Blaha, K. Schwarz, G. Madsen, D. Kvasnicka, and J. Luitz, *WIEN2k, An Augmented Plane wave+local Orbitals Program for Calculating Crystal Properties* (Karlheinz Schwarz, Techn. Universität Wien, Austria, 2001), ISBN 3-9501031-9501031-9501032.

[37] T. Sugimoto *et al.*, *J. Phys. Conf. Series* 500, 192018 (2014).

[38] C. J. Pickard and R. J. Needs, Nat. Phys. **3**, 473 (2007).
[39] G. Gao, A. R. Oganov, P. Li, Z. Li, H. Wang, T. Cui, Y. Ma, A. Bergara, A. O. Lyakhov, T. Iitaka *et al.*, Proc. Natl. Acad. Sci. **107**, 1317 (2010).
[40] R. Golser, H. Gnaser, W. Kutschera, A. Priller, P. Steier, A. Wallner, M. Čížek, J. Horáček, and W. Domcke, Phys. Rev. Lett. **94**, 223003 (2005).
[41] H. Gnaser and R. Golser, Phys. Rev. A **73**, 021202 (2006).
[42] W. Wang, A. K Belyaev, Y. Xu, A. Zhu, C. Xiao, and X.-F. Yang, Chem. Phys. Lett. **377**, 512 (2003).
[43] Z. Wang, H. Wang, J. S. Tse, T. Iitaka, and Y. Ma, Chem. Sci. **6**, 522 (2015).
[44] J. Hooper , B. Altintas, A. Shamp, and E. Zurek, J. Phys. Chem. C **117**, 2982 (2013).
[45] J. Hooper and E. Zurek, Chem. Eur. J. **18**, 5013 (2012).
[46] F.-C. Hsu , J.-Y. Luo, K.-W. Yeh, T.-K. Chen, T.-W. Huang, P. M. Wu, Y.-C. Lee, Y.-L. Huang, Y.-Y. Chu, D.-C. Yan *et al.*, Proc. Natl. Acad. Sci. **105**, 14262 (2008).
[47] A. Simon, Angewandte Chemie International Edition **36**, 1788 (1997).
[48] The carrier density (n) is evaluated through integrating the product of corresponding density of states and the Fermi-Dirac distribution function within the energy window of ~25 meV (the thermal energy at room temperature) centered at the Fermi level. As customary, we convert n to the dimensionless parameter r_s via the standard expression $4\pi r_s^3/3 = 1/n$. The r_s (in the unit of Bohr radius) refers to the radius of a sphere whose volume is equal to the volume per conducting electron.
[49] N. W. Ashcroft, Phys. Rev. Lett. **21**, 1748 (1968).
[50] P. B. Allen and R. C. Dynes, Phys. Rev. B **12**, 905 (1975).
[51] W. L. McMillan, Phys. Rev., **167**, 331 (1968).
[52] A. Y. Liu, I. I. Mazin, and J. Kortus, Phys. Rev. Lett. **87**, 087005 (2001).
[53] H. Suhl, B. T. Matthias, and L. R. Walker, Phys. Rev. Lett. **3**, 552 (1959).